Rab3A and Rab27A cooperatively regulate the docking step of dense-core vesicle exocytosis in PC12 cells

Takashi Tsuboi[1] and Mitsunori Fukuda[1,2,*]

[1]Fukuda Initiative Research Unit, RIKEN (The Institute of Physical and Chemical Research), 2-1 Hirosawa, Wako, Saitama 351-0198, Japan
[2]Laboratory of Membrane Trafficking Mechanisms, Department of Developmental Biology and Neurosciences, Graduate School of Life Sciences, Tohoku University, Aobayama, Aoba-ku, Sendai, Miyagi 980-8578, Japan
*Author for correspondence (e-mail: nori@mail.tains.tohoku.ac.jp)

Accepted 21 February 2006
Journal of Cell Science 119, 2196-2203 Published by The Company of Biologists 2006
doi:10.1242/jcs.02962

Summary

Recent studies have suggested that two small GTPases, Rab3A and Rab27A, play a key role in the late steps of dense-core vesicle exocytosis in endocrine cells; however, neither the precise mechanisms by which these two GTPases regulate dense-core vesicle exocytosis nor the functional relationship between them is clear. In this study, we expressed a number of different Rab proteins, from Rab1 to Rab41 in PC12 cells and systematically screened them for those that are specifically localized on dense-core vesicles. We found that four Rabs (Rab3A, Rab27A, Rab33A, Rab37) are predominantly targeted to dense-core vesicles in PC12 cells, and that three of them (Rab3A, Rab27A, Rab33A) are endogenously expressed on dense-core vesicles. We further investigated the effect of silencing each Rab with specific small interfering RNA on vesicle dynamics by total internal reflection fluorescence microscopy in a single PC12 cell. Silencing either Rab3A or Rab27A in PC12 cells significantly decreased the number of dense-core vesicles docked to the plasma membrane without altering the kinetics of individual exocytotic events, whereas silencing of Rab33A had no effect at all. Simultaneous silencing of Rab3A and Rab27A caused a significantly greater decrease in number of vesicles docked to the plasma membrane. Our findings indicate that Rab3A and Rab27A cooperatively regulate docking step(s) of dense-core vesicles to the plasma membrane.

Supplementary material available online at
http://jcs.biologists.org/cgi/content/full/119/11/2196/DC1

Key words: Exocytosis, Rab3A, Rab27A, Small interfering RNA, Total internal reflection fluorescence microscopy

Introduction

The release of neurotransmitters and peptide hormones involves exocytotic fusion of secretory vesicles with the plasma membrane. Although the precise mechanism that allows the fine-tuning of exocytosis is still not well understood, a variety of exocytosis-regulating proteins have recently been identified, including SNAREs (soluble *N*-ethylmaleimide-sensitive factor attachment protein receptors), VAMP-2/synaptobrevin-2, SNAP-25 (synaptosome-associated protein of 25 kDa), syntaxin-1a and Rab GTPases (Jahn and Südhof, 1999; Rothman, 1994). Rab proteins are monomeric GTPases of the Ras superfamily, which, together with their specific effector molecules, regulate multiple steps of vesicle transport, including vesicle motility, vesicle docking to specific compartments in cells and a membrane-fusion process (Pfeffer, 2001; Segev, 2001; Zerial and McBride, 2001). More than 60 distinct Rab proteins have been identified in mice and humans, and these proteins appear to regulate various types or steps of membrane trafficking (Zerial and McBride, 2001).

Recent evidence has indicated that Rab3A and Rab27A, two closely related Rab isoforms, are associated with secretory vesicles and involved in the regulation of exocytosis. First, Rab3A, Rab27A, and their effectors (i.e. Slp4-a/granuphilin-a, Slac2-c/MyRIP, Noc2, rabphilin and Rimα) are endogenously expressed in certain neuroendocrine cells (Cheviet et al., 2004a; Chung et al., 1995; Desnos et al., 2003; Fukuda et al., 2002; Fukuda et al., 2004; Regazzi et al., 1996; Waselle et al., 2003; Yi et al., 2002). Second, overexpression of Rab3A or Rab27A effectors (or their Rab-binding domain) modulates dense-core vesicle exocytosis in neuroendocrine cells (Cheviet et al., 2004a; Chung et al., 1995; Coppola et al., 2002; Desnos et al., 2003; Fukuda et al., 2002; Fukuda, 2003b; Fukuda, 2004; Fukuda et al., 2004; Sun et al., 2001; Waselle et al., 2003; Yi et al., 2002). As an example, two Rab27A effectors, Slp4-a and Slac2-c, are present on dense-core vesicles (Desnos et al., 2003; Fukuda et al., 2002; Waselle et al., 2003; Yi et al., 2002) and overexpression of Slp4-a in PC12 cells strongly inhibits dense-core vesicle exocytosis, whereas other members of the Slp family promote instead dense-core vesicle exocytosis (Fukuda et al., 2002; Fukuda, 2003b). However, it has never been elucidated whether any Rab proteins other than Rab3A and Rab27A are involved in the control of dense-core vesicle exocytosis, and whether such Rabs, or Rab3A and Rab27A themselves, function sequentially, redundantly, cooperatively or independently in dense-core vesicle exocytosis in neuroendocrine PC12 cells.

In this study, we screened for Rab members that are specifically localized on the dense-core vesicles in PC12 cells

and found that Rab33A protein, in addition to Rab3A and Rab27A, is endogenously expressed on dense-core vesicles in PC12 cells. We further investigated the function of Rab3A, Rab27A and Rab33A in the motion of a single dense-core vesicle during exocytosis in PC12 cells by total internal reflection fluorescence (TIRF) microscopy, also called evanescent wave or evanescence microscopy (Axelrod, 1981), using vesicle-targeted fluorescent proteins (Tsuboi et al., 2000; Tsuboi et al., 2003; Tsuboi et al., 2004; Tsuboi et al., 2005; Tsuboi and Fukuda, 2005; Tsuboi and Rutter, 2003). Inhibition of Rab3A or Rab27A function by small interfering RNA (siRNA) substantially reduced the number of vesicles docked at the plasma membrane and decreased the number of single exocytotic events without affecting the kinetics of vesicle fusion. Simultaneous inhibition of Rab3A and Rab27A function by siRNA caused a further reduction in the number of vesicles docked at the plasma membrane as well as in the number of single exocytotic events. By contrast, no effect was observed in Rab33A-depleted PC12 cells. Cooperative roles of Rab3A and Rab27A in the docking step of dense-core vesicle exocytosis in PC12 cells are discussed based on our findings.

Results

Rab3A, Rab27A and Rab33A are endogenously expressed in PC12 cells and associated with dense-core vesicles

To determine how many Rab isoforms specifically localize on dense-core vesicles, we first performed a Rab-family-wide analysis by expressing our pool of Rab proteins (Rab1 to Rab41), each tagged with green fluorescent protein (GFP) in PC12 cells. If certain Rabs were specifically targeted to dense-core vesicles in NGF-differentiated PC12 cells, GFP-Rab proteins should only be present in the distal part of the neurites, the same as the endogenous Rab3A and Rab27A proteins (Fukuda et al., 2002). Only three, phylogenetically similar, proteins of this Rab1 to Rab41 group (Fukuda, 2003a; Pereira-Leal et al., 2001), i.e. Rab3A, Rab27A and Rab37, were exclusively localized in the neurites of the NGF-differentiated PC12 cells; Rab33A was predominantly localized in the neurites but also in the Golgi-like structure (supplementary material Fig. 1A). By contrast, other Rabs were mainly present in the peri-nuclear regions, plasma membrane and/or cytoplasm, rather than in the neurites (summarized in supplementary material Fig. 1B).

To further determine whether the above four Rab proteins were actually present on dense-core vesicles, we simultaneously labeled the dense-core vesicle cargo and Rab proteins in PC12 cells by expressing mutant pH-insensitive yellow fluorescent protein (YFP)-tagged neuropeptide Y (NPY-Venus), which efficiently targets dense-core vesicles (Nagai et al., 2002) and also mRFP-Rab3A, mRFP-Rab27A, mRFP-Rab33A or mRFP-Rab37. Confocal microscopy showed that most NPY-Venus-positive vesicles (74.6±3.6%, n=5 cells) colocalized with mRFP-Rab3A-positive vesicles (Fig. 1A-C), confirming the efficient targeting of mRFP-Rab3A to NPY-positive vesicles (i.e. dense-core vesicles). Similarly, most mRFP-Rab27A-labeled (Fig. 1D-F; 87.6±2.6%, n=5 cells), mRFP-Rab33A-labeled (Fig. 1G-I, 94.5±4.6%, n=5 cells) and mRFP-Rab37-labeled (Fig. 1J-L, 79.3±5.2%, n=5 cells) structures colocalized with NPY-Venus. Endogenous expression of Rab3A, Rab27A, Rab33A and Rab37 in PC12 cells was finally determined by immunoblotting with specific antibodies (Fig. 2). Expression of Rab3A, Rab27A and Rab33A proteins in PC12 cells was readily detected, but no expression of Rab37 protein was observed under our experimental conditions (Fig. 2, lane 6).

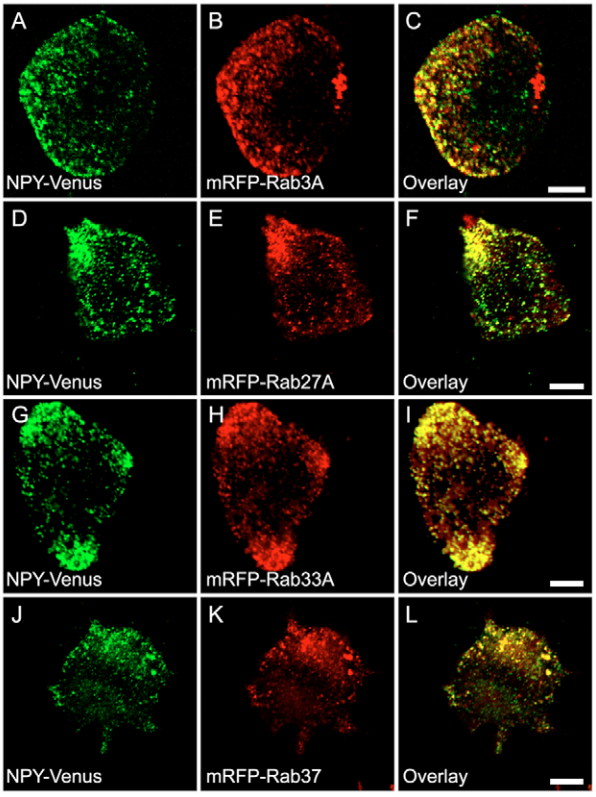

Fig. 1. Colocalization of Rab proteins with secretory vesicles in PC12 cells. NPY-Venus (A,D,G,J) and mRFP-Rab3A (B), mRFP-Rab27A (E), mRFP-Rab33A (H) or mRFP-Rab37 (K) were coexpressed in PC12 cells, and images of the fixed cells were obtained by confocal microscopy. Note that all four mRFP-Rabs colocalized well with the dense-core vesicle marker NPY-Venus. Bars, 5 μm.

Silencing of Rab3A, Rab27A and Rab33A proteins with specific siRNAs

To investigate the role(s) of Rab3A, Rab27A and Rab33A proteins in PC12 cells, endogenous expression of Rab3A, Rab27A and Rab33A proteins was reduced with specific siRNAs against each Rab isoform (see Materials and Methods for details). The effect of the siRNAs on the number of plasma-membrane-docked dense-core vesicles and number of exocytotic responses was monitored by TIRF microscopy (Tsuboi et al., 2000; Tsuboi et al., 2004; Tsuboi et al., 2005; Tsuboi and Fukuda, 2005; Tsuboi and Rutter, 2003). Expression of the Rab3A, Rab27A and Rab33A siRNAs reduced endogenous expression of Rab3A (Fig. 3A, 85.7±4.7%, n=3), Rab27A (Fig. 3C, 72.4±5.6%, n=3) and Rab33A (Fig. 3E, 61.3±10.4%, n=3), respectively, in PC12 cells by 48 hours after transfection, but their expression levels were unaffected when cells were transfected with a pSilencer vector as a control (Fig. 3A,C,E). To verify at single-cell level the effect of these siRNAs on endogenous expression of their

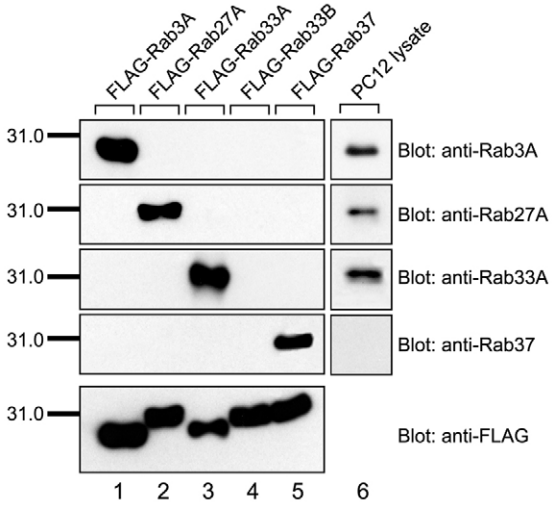

Fig. 2. Expression of Rab3A, Rab27A and Rab33A in PC12 cells. The same amount of recombinant FLAG-tagged Rab3A, Rab27A, Rab33A, Rab33B or Rab37 expressed in COS-7 cells (lanes 1-5) and total homogenates of PC12 cells (20 μg, lane 6) were loaded on 10% SDS-PAGE and immunoblotted with HRP-conjugated anti-FLAG (bottom panel), anti-Rab3A-, anti-Rab27A-, anti-Rab33A-, or anti-Rab37-specific antibody. Note that each of the four antibodies specifically recognized a single Rab isoform, and that Rab3A, Rab27A and Rab33A are endogenously expressed in PC12 cells. The positions of the molecular mass markers ($\times 10^{-3}$) are shown on the left.

respective Rabs, we co-transfected the siRNAs together with a pEGFP-C1 vector as a transfection marker and examined them with an immunofluorescence microscope. Marked reductions of endogenous Rab3A, Rab27A and Rab33A signals by their respective siRNA were also observed in approximately 65% of the GFP-expressing PC12 cells (n>130 cells, six dishes per each experiment) (see Fig. 3B,D,F, arrowheads).

Silencing of Rab3A or Rab27A by siRNA reduces the number of secretory vesicles docked at the plasma membrane and the number of exocytotic events

To explore the possible role of Rab3A, Rab27A and Rab33A in dense-core vesicle exocytosis (e.g. recruitment, docking and fusion), we silenced Rab proteins with siRNAs and monitored by TIRF microscopy the impact of silencing on the dynamics of single exocytotic events within ~100 nm beneath the plasma membrane of PC12 cells (Axelrod, 1981; Tsuboi et al., 2000; Tsuboi et al., 2003; Tsuboi et al., 2004; Tsuboi et al., 2005; Tsuboi and Fukuda, 2005; Tsuboi and Rutter, 2003). This was accomplished by labeling dense-core vesicles with NPY-Venus and counting the number of plasma membrane-associated vesicles in the presence of specific siRNAs by TIRF microscopy before stimulating the cells with high-KCl solution (70 mM). We

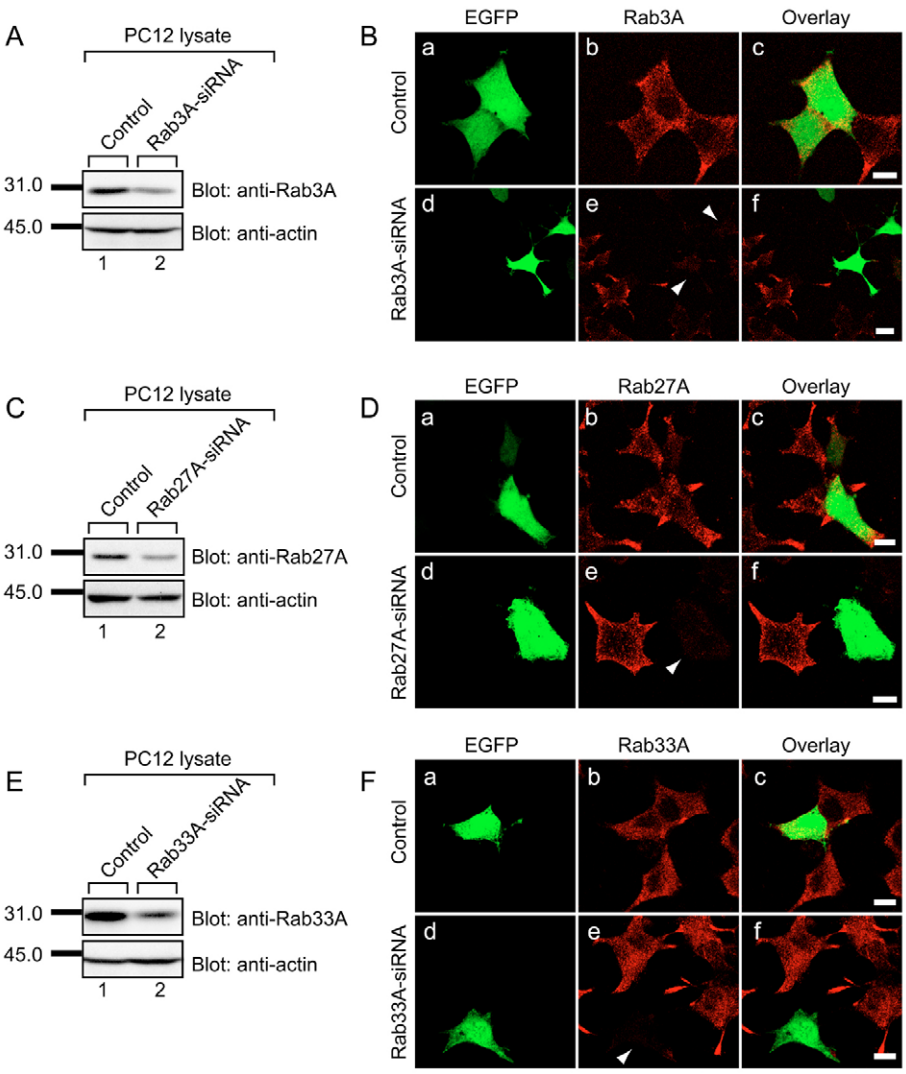

Fig. 3. Silencing of endogenous Rab3A, Rab27A, and Rab33A with specific siRNAs. PC12 whole-cell lysates were prepared 2 days after transfection with Rab3A-siRNA (A), Rab27A-siRNA (C) or Rab33A-siRNA (E) as described in Materials and Methods. The knockdown effect of the siRNAs on endogenous expression of Rabs was evaluated by immunoblot analysis with specific antibodies (see also Fig. 2). The positions of the molecular mass markers ($\times 10^{-3}$) are shown on the left. (B) PC12 cells transiently co-transfected with pEGFP-C1 and with a control vector (a-c) or with a vector containing Rab3A-siRNA (d-f). (D) PC12 cells transiently co-transfected with pEGFP-C1 and with a control vector (a-c) or with a vector containing Rab27A-siRNA (d-f). (F) PC12 cells transiently co-transfected with pEGFP-C1 and with a control vector (a-c) or with a vector containing Rab33A-siRNA (d-f). Note that expression of the specific siRNAs dramatically reduced endogenous expression of the Rab proteins (see arrowheads in panel e of B,D,F). Bars, 10 μm.

first investigated the transfection efficiency of the siRNAs in NPY-Venus-expressing PC12 cells by immunofluorescence analysis. We found that 68.3±5.7%, 66.3±1.3% and 67.5±4.3% of NPY-Venus-expressing PC12 cells (n>125 cells, six dishes per experiment) showed a significant reduction of endogenous Rab3A, Rab27A and Rab33A signals, respectively (see also Fig. 3), indicating a high transfection efficiency when NPY-Venus and siRNAs were co-transfected. As shown in Fig. 4A, expression of either Rab3A or Rab27A siRNA, significantly reduced the number of plasma-membrane-docked vesicles (by 70.1% and 61.4%, respectively) (Fig. 4B), whereas expression of Rab33A siRNA had no effect. These effects are unlikely to be attributable to the differences in NPY-Venus expression levels in the Rab3A, Rab27A and Rab33A siRNA-expressing cells, because NPY-Venus expression levels did not differ much (inset in Fig. 4B).

We next counted the total number of NPY-Venus release events in cells that express NPY-Venus together with either Rab3A, Rab27A or Rab33A siRNA during incubation with the high-KCl buffer. The number of NPY-Venus release events was reduced by 57.8% and 42.8% in Rab3A-siRNA-expressing and Rab27A-siRNA-expressing cells, respectively, compared with the control cells (Fig. 4C). Again, expression of the Rab33A-siRNA had no effect.

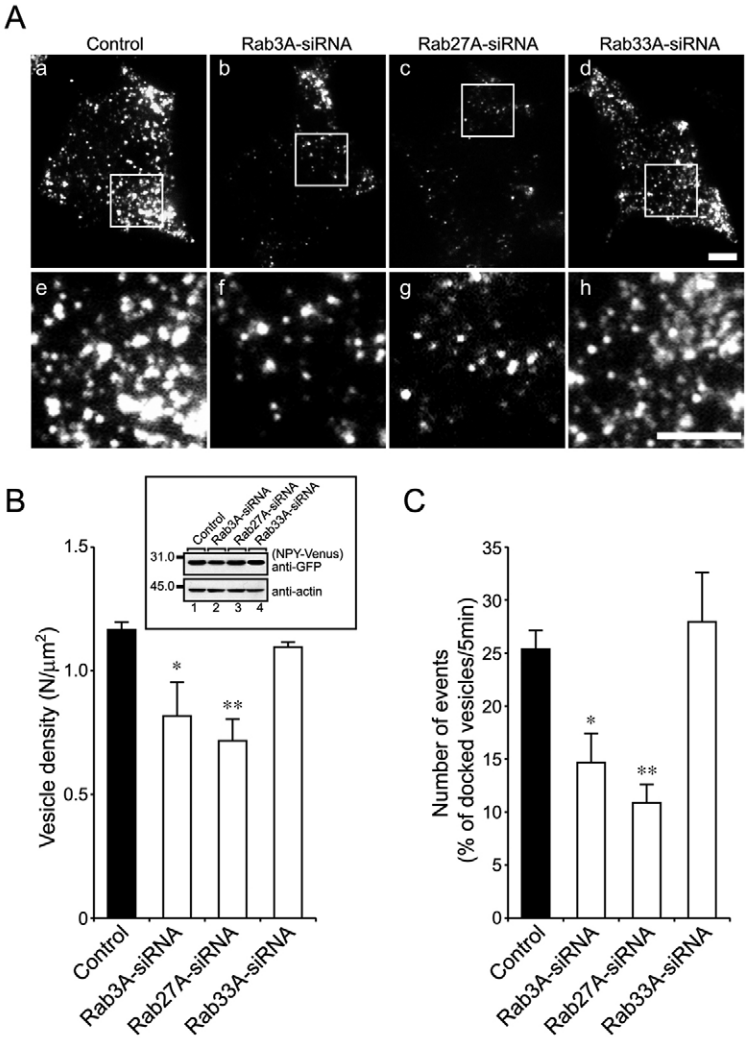

Fig. 4. Effect of siRNA expression on the number of vesicles docked to the plasma membrane in PC12 cells. (A) Typical TIRF images of plasma membrane-docked vesicles before high-KCl stimulation of control (a), Rab3A-siRNA-expressing (b), Rab27A-siRNA-expressing (c) and Rab33A-siRNA-expressing cells (d). (e-h) Magnified images of the boxed area. Bars, 5 μm. (B) The density of docked vesicles was determined by counting the vesicles in each image (n=6 cells in each). The inset shows NPY-Venus and actin protein expression visualized with anti-GFP and anti-actin antibody, respectively. The positions of the molecular mass markers ($\times 10^{-3}$) are shown on the left. (C) The number of NPY-Venus spot disappearance events was counted as fusion events in a 5-minute period (n=6 cells in each). The data are mean values ± s.e.m. and were analyzed by one-way ANOVA followed by Newman-Keuls multiple comparison test. *P<0.05 and **P<0.01, respectively, compared with the control. Note that expression of either Rab3A or Rab27A siRNA significantly reduced the number of plasma membrane-docked vesicles (B) as well as the number of NPY-Venus release events (C).

Effect of silencing Rab3A or Rab27A on vesicle fusion

To determine whether silencing of Rab3A or Rab27A inhibits the rate (or kinetics) of vesicle exocytosis, the dynamics of single-vesicle fusion events was analyzed in single NPY-Venus-expressing vesicles near the plasma membrane. Although exocytotic events were detected much less frequently in cells that expressed Rab3A or Rab27A siRNA compared with control cells or cells transfected with Rab33A siRNA (Fig. 4C), the kinetics of individual fusion events was identical in all cells (Fig. 5): stimulation with high-KCl buffer caused NPY-Venus-containing spots to brighten and expand suddenly during the release of the fluorescent peptide (Tsuboi et al., 2004), with an identical time course in all cells (Fig. 5B). Thus, these results strongly indicate that Rab3A and Rab27A regulate the docking of dense-core vesicles to the plasma membrane in PC12 cells, rather than modulate vesicle fusion (or the kinetics of vesicle fusion) itself.

Effect of simultaneous silencing of Rab3A and Rab27A on the number of secretory vesicles docked at the plasma membrane, and the number of exocytotic events

Although most Rab3A-positive vesicles colocalized with Rab27A-positive vesicles (Fig. 6A) (96.7±3.4%, n=3), Rab3A (or Rab27A) cannot completely compensate for the function of Rab27A (or Rab3A) in Rab27A-depleted (or Rab3A-depleted) PC12 cells, suggesting that Rab3A and Rab27A differentially contribute to the control of dense-core vesicle exocytosis. To explore the functional relationship between Rab3A and Rab27A (e.g. sequential function or cooperative function) in dense-core vesicle exocytosis, we investigated the effect of simultaneous silencing of Rab3A and Rab27A on the docking of dense-core vesicles to the plasma membrane by TIRF microscopy. Efficiency of double knockdown of endogenous Rab3A and Rab27A (62.1±4.1%; n=143 cells, six dishes per experiment) in NPY-Venus-expressing PC12 cells was almost similar to that of the single knockdown of Rab3A (68.3±5.7%) or Rab27A (66.3±1.3%) described above. Simultaneous silencing of Rab3A and Rab27A proteins dramatically decreased the number of plasma membrane-docked vesicles

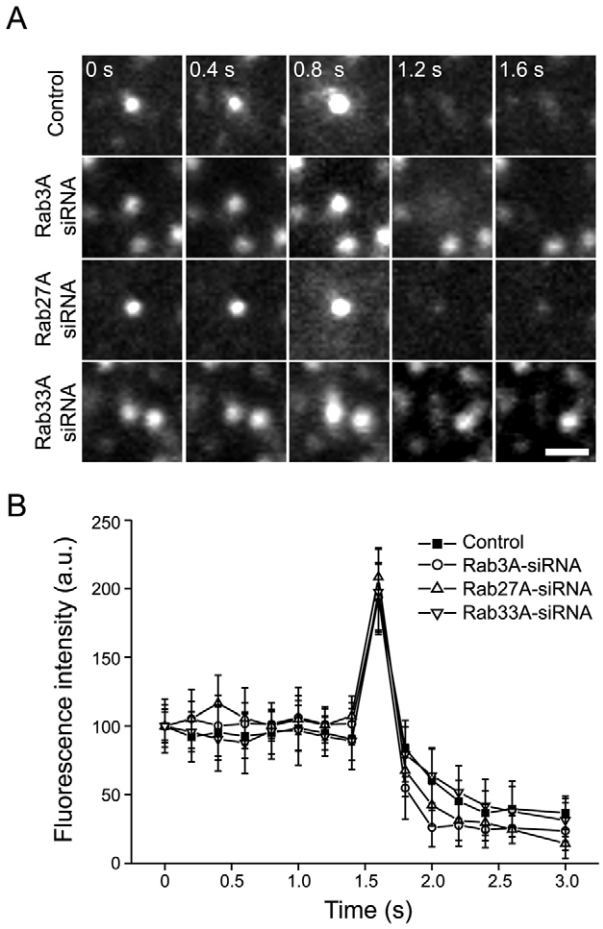

Fig. 5. Effect of the Rab3A-siRNA, Rab27A-siRNA, and Rab33A-siRNA expression on the kinetics of NPY-Venus release. (A) Typical sequential images of a single NPY-Venus vesicle observed after high-KCl (70 mM) stimulation of cells expressing control vector (control), Rab3A-siRNA (Rab3A siRNA), Rab27A-siRNA (Rab27A siRNA) or Rab33A-siRNA (Rab33A siRNA), acquired at 200-millisecond intervals, through a TIRF microscope. The third column of images (0.8 seconds) shows a diffuse cloud of NPY-Venus fluorescence, and the fourth column of images (1.2 second) shows disappearance of the spot. (B) Time course of the fluorescence changes measured in the center of NPY-Venus vesicles in the control (■), Rab3A-siRNA-expressing (○), Rab27A-siRNA-expressing (△), and Rab33A-siRNA-expressing (▽) cells. Mean fluorescence intensity before fusion was set as 100% (n=15 vesicles in each experiment). Bar, 2 μm. Images were acquired every 200 milliseconds under each set of conditions. Note that silencing Rab3A, Rab27A, or Rab33A had no effect on the kinetics of vesicle fusion of the dense-core vesicles.

(Fig. 6B, right panels), compared with the control cells (Fig. 6B, left panels). Quantitative analysis by TIRF microscopy indicated that simultaneous depletion of Rab3A and Rab27A proteins caused a dramatic reduction (by 43.9%) of the number of plasma membrane-docked vesicles in PC12 cells to a level significantly lower than that in the single Rab-depleted PC12 cells (Fig. 6C). Similarly, the number of NPY-Venus release events was dramatically reduced by 35.7% in Rab3A/Rab27A-depleted PC12 cells, which is significantly lower than in the single Rab3A-depleted PC12 cells (Fig. 6D). The number of NPY-Venus release events in the Rab3A/Rab27A-depleted cells was also slightly lower than that in the single Rab27A-depleted cells, but this difference was not significant under our experimental conditions (Fig. 6D). Taken together, these findings suggest that Rab3A and Rab27A regulate the docking step of dense-core vesicles to the plasma membrane in PC12 cells cooperatively rather than sequentially.

Discussion

In the present study we demonstrated for the first time that four Rab isoforms (Rab3A, Rab27A, Rab33A, Rab37) tagged with GFP are mainly targeted to dense-core vesicles in PC12 cells, and that three of them, Rab3A, Rab27A and Rab33A, are endogenously expressed on the dense-core vesicles of PC12 cells (Fig. 2). We also demonstrated by TIRF microscopy combined with RNA interference technology that both Rab3A and Rab27A are involved in the control of the docking step of dense-core vesicle exocytosis rather than in the kinetics of vesicle fusion (Figs 4-6). Although Rab3A and Rab27A are present on the same dense-core vesicles (Fig. 6A), we came to the following two conclusions why they are unlikely to function redundantly or sequentially in dense-core vesicle exocytosis. First, siRNA-mediated knockdown of Rab3A (or Rab27A) reduced the number of vesicles docked to the plasma membrane, and endogenous Rab27A (or Rab3A) was unable to fully compensate the function of Rab3A (or Rab27A) (Fig. 4), suggesting that the functions of Rab3A and Rab27A are not completely redundant. Second, double knockdown of Rab3A and Rab27A resulted in a more severe docking defect than single knockdown (Fig. 6), suggesting that Rab3A and Rab27A do not function sequentially in the process of dense-core vesicle exocytosis, and that both are involved in the control of the same docking step of exocytosis. Involvement of Rab27A in the vesicle docking step in PC12 cells is quite consistent with previous reports in other secreting cells (Haddad et al., 2001; Kasai et al., 2005; Stinchcombe et al., 2001).

How do Rab3A and Rab27A cooperatively regulate the docking step of dense-core vesicle exocytosis? We think that the cooperative function of Rab3A and Rab27A might be explained by the diversity of Rab3A and Rab27A effectors expressed in endocrine cells (Cheviet et al., 2004b; Fukuda, 2005). At least seven Rab3A/27A effectors (Rim1/2, rabphilin, Noc2, Slp4-a, Slp5 and Slac2-c) were already shown to be expressed in certain endocrine cells (Fukuda, 2005). Interestingly, rabphilin and Noc2, previously characterized as Rab3A effectors (Haynes et al., 2001; Kotake et al., 1997; Shirataki et al., 1993), also function as Rab27A effectors (Cheviet et al., 2004a; Fukuda et al., 2004), and the Rab27A effector Slp4-a can interact with Rab3A (Coppola et al., 2002; Fukuda et al., 2002; Kuroda et al., 2002a; Yi et al., 2002). It has recently been proposed that Slp4-a promotes the docking of dense-core vesicles to the plasma membrane by simultaneously interacting with Rab27A on the vesicle and with syntaxin-1a/Munc18-1 on the plasma membrane (Coppola et al., 2002; Fukuda, 2003b; Fukuda et al., 2005; Torii et al., 2004), and that rabphilin controls the docking step of dense-core vesicle exocytosis by simultaneously interacting with Rab27A on the vesicle and with SNAP-25 on the plasma membrane (Fukuda, 2006; Tsuboi and Fukuda, 2005) (see Fig. 7). Further studies are needed to determine the exact function of Rab3A and/or Rab27A effectors in the dense-core vesicle docking step.

We found that two other Rabs, Rab33A and Rab37, in

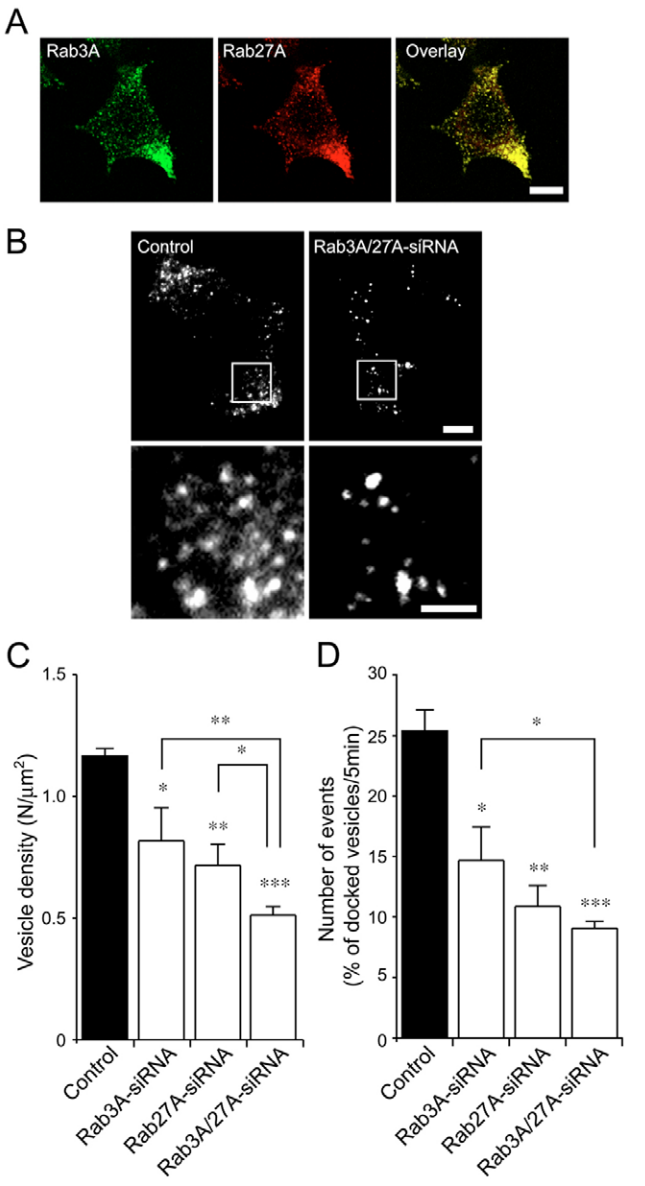

Fig. 6. Effect of simultaneous silencing of Rab3A and Rab27A on the number of vesicles docked to the plasma membrane in PC12 cells. (A) Confocal images of a PC12 cell showing colocalization of endogenous Rab3A (green signals in the left panel) and Rab27A (red signals in the middle panel). The right panel shows the overlay between Rab3A and Rab27A (yellow signals in the right panel). Scale bar=10 μm. (B) Typical TIRF images of plasma membrane-docked vesicles in a control cell (left) and a Rab3A- and Rab27A-siRNA-expressing cell (right). The bottom panels are magnified images of the boxed area. Scale bar=5 μm. (C) The density of docked vesicles was determined by counting the vesicles in each image (n=6 cells in each). (D) The number of NPY spot disappearance events in 5 minutes was counted as fusion events (n=6 cells in each). Data shown are mean values ± s.e.m. and were analyzed by one-way ANOVA followed by Newman-Keuls multiple comparison test. *P<0.05, **P<0.01, and ***P<0.001, respectively, in comparison with the control. Note that simultaneous silencing of Rab3A and Rab27A caused a significant reduction of vesicle density than silencing of Rab3A or Rab27A alone.

addition to Rab3A and Rab27A, are mainly targeted to dense-core vesicles when expressed in PC12 cells (Fig. 1). Endogenous expression of Rab37 was not detected in PC12 cells, and no effect of overexpression of Rab37 in PC12 cells on dense-core vesicle exocytosis was detected by TIRF microscopy (data not shown). Since Rab37 is exclusively expressed in mast cells (Masuda et al., 2000), the lack of any effect of Rab37 expression on dense-core vesicle exocytosis may be explained by the notion that Rab37 effector(s) are not endogenously expressed in PC12 cells. It would be interesting to investigate the function of Rab37 in the docking process of histamine-containing granules in mast cells. Although Rab33A is endogenously expressed in PC12 cells, our results indicate that Rab33A is not involved in the late stages of dense-core vesicle exocytosis. Since Rab33A signals have also been found in Golgi-like structures (Zheng et al., 1998) in addition to dense-core vesicles, a possible function of Rab33A is to facilitate post-Golgi trafficking, which may promote delivery of immature secretory vesicles to the cell periphery. Alternatively, Rab33A might be involved in the control of endosome-to-Golgi transport and/or retrograde transport from late to early Golgi compartments (Zheng et al., 1998). Further studies are needed to determine the exact function of Rab33A in membrane trafficking in PC12 cells.

In summary, we have demonstrated that both Rab3A and Rab27A are present on the same dense-core vesicles in PC12 cells, and cooperatively regulate the docking step of dense-core vesicle exocytosis in PC12 cells. As far as we know, this is the first study to demonstrate a functional relationship between Rab3A and Rab27A in regulated exocytosis. Future studies on

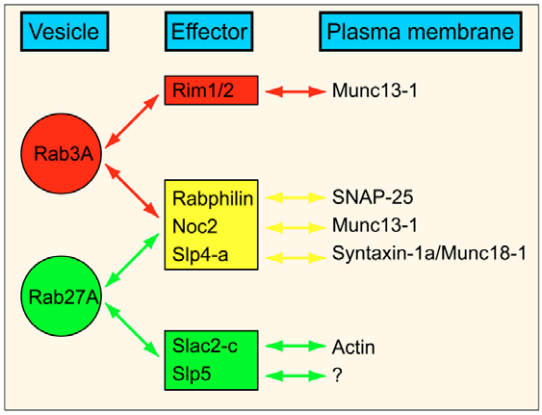

Fig. 7. Hypothetical model of dense-core vesicle docking mediated by Rab3A, Rab27A,and their effectors. At least seven Rab effectors (Rim1α, Rim2α, rabphilin, Noc2, Slp4-a, Slp5 and Slac2-c) are known to be expressed in endocrine cells. Three of them (rabphilin, Noc2 and Slp4-a) are capable of interacting with both Rab3A and Rab27A (Coppola et al., 2002; Fukuda et al., 2002; Haynes et al., 2001; Kotake et al., 1997; Kuroda et al., 2002a; Shirataki et al., 1993; Yi et al., 2002), whereas Rim interacts only with Rab3A (Fukuda, 2004; Fukuda, 2003a); Slac2-c and Slp5 specifically interact with Rab27A (Fukuda and Kuroda, 2002; Kuroda et al., 2002b). These Rab effectors simultaneously bind Rab27A on vesicle and plasma membrane proteins, plasma membrane-associated proteins or actin (see the text for details), and might be involved in the docking of dense-core vesicles to the plasma membrane (An and Almers, 2004; Betz et al., 2001; Cheviet et al., 2004a; Coppola et al., 2002; Desnos et al., 2003; Fukuda et al., 2003b; Fukuda et al., 2005; Imai et al., 2004; Torii et al., 2004; Tsuboi and Fukuda, 2005; Waselle et al., 2003).

the roles of Rab3A and Rab27A effectors will clarify the mechanism by which the two exocytotic Rabs cooperatively regulate the docking step of dense-core vesicle exocytosis at the molecular level.

Materials and Methods

Materials

Anti-Rab3A and Anti-Rab27A mouse monoclonal antibodies were obtained from BD Transduction Laboratories (Lexington, KY). Anti-GFP mouse monoclonal antibody and anti-actin goat polyclonal antibody were obtained from BD Clontech (Palo Alto, CA) and Santa Cruz Biotechnology, Inc. (Santa Cruz, CA), respectively. Horseradish peroxidase (HRP)-conjugated anti-FLAG M2 mouse monoclonal antibody, HRP-conjugated goat anti-mouse IgG, and HRP-conjugated goat anti-rabbit IgG were from Sigma Chemical Co (St Louis, MO). Fluorescent-dye-conjugated secondary antibodies (Alexa Fluor 488-labeled anti-mouse and Alexa Fluor 568-labeled anti-mouse or anti-rabbit IgGs) were from Molecular Probes Inc. (Eugene, OR). Anti-Rab27A, anti-Rab33A and anti-Rab37 rabbit polyclonal antibody were prepared as described previously with glutathione *S*-transferase (GST)-Rab27A, GST-Rab33A and GST-Rab37, respectively, as an antigen (Fukuda and Mikoshiba, 1999; Imai et al., 2004).

Plasmid construction

The following pairs of nucleotides with a 19-base target site (bold) and a 9-base loop (italics) were used to generate siRNA-expression plasmids against rat Rab3A or Rab33A mRNA. Rab3A siRNA(+) primer (5′-**GGACAACATTAATGTCAAG-***TTCAAGAGA***CTTGACATTAATGTTGTCCTTTTTT-3′) and Rab3A siRNA(–) primer (5′-AATTAAAAAA**GGACAACATTAATGTCAAG***TCTCTTGAA*CTTG-ACATTAATGTTGTCCGGCC-3′) for Rab3A siRNA; and Rab33A siRNA(+) primer (5′-**ATCCCTCTTGTACCGTGAT***TTCAAGAGA*ATCACGGTACAAGA-GGGATTTTTTT-3′) and Rab33A siRNA (–) primer (5′-AATTAAAAAA-**ATCCCTCTTGTACCGTGAT***TCTCTTGAA*ATCACGGTACAAGAAGGATGG-CC-3′) for Rab33A siRNA. The pairs of nucleotides were mixed, denatured at 94°C for 2 minutes, annealed at 72°C for 1 minute, gradually cooled to 4°C for 2 hours, and then subcloned into the *Apa*I and *Eco*RI sites of the pSilencer 1.0-U6 vector (Ambion, Austin, TX), which expresses short hairpin RNA under the control of the mouse U6 promoter. The plasmids obtained were referred to as pSilencer-Rab3A and pSilencer-Rab33A, respectively.

The Rab3A, Rab27A, Rab33A and Rab37 cDNA fragments (Fukuda, 2003a; Kuroda et al., 2002a) were subcloned into the *Bam*HI/*Not*I site of the pmRFP-C1-gk vector (Tsuboi and Fukuda, 2005) modified from pmRFP-C1 (BD Clontech), by introducing a short Gly linker immediately downstream from mRFP (monomeric red fluorescent protein) (Campbell et al., 2002). Plasmid encoding NPY (neuropeptide Y)-Venus (pVenus-N1-NPY) was generously provided by Atsushi Miyawaki (Nagai et al., 2002). Other expression constructs (pEF-FLAG-Rab3A, pEF-FLAG-Rab27A, pEF-FLAG-Rab33A, pEF-FLAG-Rab33B, pEF-FLAG-Rab37, pSilencer-Rab27A and pEGFP-C1-Rabs) were prepared as described elsewhere (Fukuda, 2003a; Kuroda et al., 2002a; Kuroda and Fukuda, 2004; M.F., unpublished data).

Cell culture

PC12 cells were cultured in Dulbecco's modified Eagle's medium (DMEM) supplemented with 10% fetal bovine serum, 10% horse serum, 100 U/ml penicillin G, and 100 μg/ml streptomycin, at 37°C under 5% CO_2 (Fukuda et al., 2002). For differentiation of PC12 cells, the cells were treated with 100 ng/ml β-nerve growth factor (NGF). COS-7 cells were cultured in DMEM supplemented with 10% fetal bovine serum, 100 U/ml penicillin G, and 100 μg/ml streptomycin.

Immunoblotting

PC12 cells (one confluent 10-cm dish) were homogenized in buffer containing 1 ml of 50 mM HEPES-KOH pH 7.2, 150 mM NaCl, 0.5 mM GTPγS[guanosine 5′-O-(3-thiotriphosphate)] and protease inhibitors (0.1 mM phenylmethylsulfonyl fluoride, 10 μM leupeptin, and 10 μM pepstatin A) in a glass-Teflon Potter homogenizer by 10 strokes at 900-1000 rpm. After solubilization with 1% Triton X-100 at 4°C for 1 hour, the insoluble material was removed by centrifugation at 15,000 rpm for 10 minutes. The proteins were analyzed by 10% SDS-polyacrylamide gel electrophoresis (PAGE) followed by immunoblotting with anti-Rab3A mouse monoclonal antibody (1:250 dilution), anti-Rab27A mouse monoclonal antibody (1:1000 dilution), anti-Rab33A rabbit polyclonal antibody (1 μg/ml) and anti-Rab37 rabbit polyclonal antibody (4 μg/ml). Immunoreactive bands were visualized with HRP-conjugated goat anti-mouse IgG (1:10,000) or HRP-conjugated goat anti-rabbit IgG (1:10,000) and detected by enhanced chemiluminescence (ECL) (Amersham Biosciences, Buckinghamshire, UK).

pEF-FLAG-Rab vectors (4 μg of plasmids in total) were transfected into COS-7 cells (density of 7.5×10^5 cells per 10-cm dish the day before transfection) with Lipofectamine Plus reagent (Invitrogen, Carlsbad, CA) according to the manufacturer's instructions. Three days after transfection, the cells expressing FLAG-Rab3A, FLAG-Rab27A, FLAG-Rab33A or FLAG-Rab37 proteins were harvested and homogenized in 1 ml of the homogenization buffer described above. Proteins were analyzed by 10% SDS-PAGE followed by immunoblotting with HRP-conjugated anti-FLAG tag (M2) antibody (1:10,000 dilution).

RNA interference

PC12 cells cultured on a 35-mm dish were co-transfected with 3 μg of pSilencer vectors and 1 μg of pEGFP-C1 vector as a marker of transfected cells with Lipofectamine 2000 (Invitrogen) according to the manufacturer's instructions. Two days after transfection, cells were subjected to immunofluorescence analysis, and downregulation of endogenous Rab3A, Rab27A or Rab33A protein was confirmed visually. To evaluate the efficacy of the siRNA against each Rab, we counted the number of EGFP- (or NPY-Venus)-positive and endogenous Rab-negative cells and the total number of EGFP- (or NPY-Venus)-positive cells in three different observation fields of each culture dish, and then the transfection efficiency of the siRNAs was calculated. To quantitatively validate the knockdown effect of siRNA by immunoblotting, PC12 cells cultured on a 10-cm dish were co-transfected with 18 μg of pSilencer vectors and 6 μg of pEGFP-C1 vector. Two days after transfection, cell lysates were prepared as described above, and tested for expression of Rab3A, Rab27A and Rab33A with anti-Rab3A mouse monoclonal antibody (1:100 dilution), anti-Rab27A rabbit polyclonal antibody (2 μg/ml) and anti-Rab33A rabbit polyclonal antibody (2 μg/ml), respectively. Immunoreactive bands were visualized with HRP-conjugated goat anti-mouse IgG (1:10,000) or HRP-conjugated goat anti-rabbit IgG (1:10,000) and detected by ECL.

To assess whether silencing of Rab proteins affects dense-core vesicle biogenesis, we co-transfected PC12 cells (one confluent 10-cm dish) with pSilencer vectors (18 μg of plasmids in total) together with pNPY-Venus (6 μg of plasmids in total) with Lipofectamine 2000 according to the manufacturer's instructions. Three days after transfection, the cells expressing NPY-Venus together with either the Rab3A siRNA, Rab27A siRNA or Rab33A siRNA were harvested and homogenized in 1 ml of the homogenization buffer as described above. The proteins were analyzed by 10% SDS-PAGE followed by immunoblotting with anti-GFP mouse monoclonal antibody (1:250 dilution) and HRP-conjugated goat anti-mouse IgG antibody (1:10,000 dilution).

TIRF microscopy

PC12 cells were cultured as described above (Fukuda et al., 2002). For total internal reflection fluorescence (TIRF) imaging, PC12 cells were plated onto poly-L-lysine-coated coverslips. Cells were co-transfected with 1 μg of pVenus-N1-NPY and either 3 μg of pSilencer (a vector control), pSilencer-Rab3A, pSilencer-Rab27A or pSilencer-Rab33A with Lipofectamine 2000 according to the manufacturer's instructions. For double knockdown of Rab3A and Rab27A, cells were triple-transfected with 1 μg of pVenus-N1-NPY, 3 μg of pSilencer-Rab3A and 3 μg of pSilencer-Rab27A. The imaging was performed in modified Ringer's buffer at 37°C (RB: 130 mM NaCl, 3 mM KCl, 5 mM $CaCl_2$, 1.5 mM $MgCl_2$, 10 mM glucose, and 10 mM HEPES pH 7.4). Stimulation with high-KCl buffer was achieved by perfusion with RB containing 70 mM KCl (NaCl was reduced to maintain the osmolarity).

Exocytosis of NPY-Venus at the single-vesicle level was monitored with a TIRF microscope similar to that described previously (Tsuboi et al., 2000; Tsuboi and Fukuda, 2005; Tsuboi and Rutter, 2003). In brief, a high numerical aperture objective lens (Plan Apochromatic, 100×, NA=1.45, infinity corrected, Olympus, Tokyo, Japan) was mounted on an inverted microscope (IX81, Olympus). The incident light for total internal reflection illumination was introduced into the high numerical aperture objective lens through a single-mode optical fiber and two illumination lenses (IX2-RFAEVA-2, Olympus). To observe the NPY-Venus fluorescence image, we used a diode-pumped solid-state 488-nm laser (HPU50100, 20 mW, Furukawa Electronic, Chiba, Japan) for total internal fluorescence illumination and a band-pass filter (HQ535/30m, Chroma, Rockingham, VT) as an emission filter. The laser beam was passed through an electromagnetically driven shutter (VMM-D3J, Unibritz, Rochester, NY). The shutter was opened synchronously with an electron multiplier charge-coupled device camera (C9100-02, Hamamatsu Photonics, Hamamatsu, Japan), and the length of exposure was controlled by MetaMorph software (version 6.3, Universal Imaging Corporation, Downingtown, PA). Images were acquired every 400 milliseconds or as indicated. To analyze the TIRF imaging data, single exocytotic events were manually selected, and the average fluorescence intensity of individual vesicles in a 0.7 μm × 0.7 μm square placed over the center of the vesicle was calculated. To define a single docked vesicle, we processed each image by high-pass filter as described in Lang et al. (Lang et al., 2000) and then counted the number of plasma-membrane-docked vesicles at the entire cell surface in the evanescent field. The number of fusion events was manually counted for a 5-minute period. Data shown are the means ± s.e.m. of at least five individual experiments. Statistical differences between means were compared by one-way ANOVA followed by Newman-Keuls multiple comparison test with GraphPad Prism software (GraphPad Software, Inc., San Diego, CA).

Confocal imaging

For microscopic analysis, PC12 cells were fixed with 4% paraformaldehyde (Wako Pure Chemicals, Osaka, Japan) for 20 minutes. For immunostaining, cells were permeabilized with 0.3% Triton X-100 for 2 minutes and blocked with blocking buffer (1% BSA and 0.1% Triton X-100 in PBS) for 1 hour. The cells were first

immunostained with the primary antibodies and then with Alexa Fluor 488- and 568-labeled secondary IgG (1:5,000 dilution). Cells were examined for fluorescence with a confocal laser-scanning microscope (Fluoview 500, OLYMPUS), and the images of the cells were processed with MetaMorph software.

We thank Atsushi Miyawaki (RIKEN Brain Science Institute, Saitama, Japan) for kindly donating NPY-Venus, and Eiko Kanno and Megumi Satoh for technical assistance. This work was supported in part by the Ministry of Education, Culture, Sports and Technology of Japan (Grants 17657067, 18022048, 18050038, 18057026 and 18207015), the Kato Memorial Bioscience Foundation, the Sumitomo Foundation and the Nakatomi Foundation (all to M.F.), by the Ministry of Education, Sports and Technology of Japan (Grant 18689008) and by the Mochida Memorial Foundation for Medical and Pharmaceutical Research, the Uehara Memorial Foundation, and the FY2005 DRI Research Grant (all to T.T.). T.T. was also supported by the Special Postdoctoral Researchers Program of RIKEN.

References

An, S. J. and Almers, W. (2004). Tracking SNARE complex formation in live endocrine cells. *Science* **306**, 1042-1046.

Axelrod, D. (1981). Cell-substrate contacts illuminated by total internal reflection fluorescence. *J. Cell Biol.* **89**, 141-145.

Betz, A., Thakur, P., Junge, H. J., Ashery, U., Rhee, J. S., Scheuss, V., Rosenmund, C., Rettig, J. and Brose, N. (2001). Functional interaction of the active zone proteins Munc13-1 and RIM1 in synaptic vesicle priming. *Neuron* **30**, 183-196.

Campbell, R. E., Tour, O., Palmer, A. E., Steinbach, P. A., Baird, G. S., Zacharias, D. A. and Tsien, R. Y. (2002). A monomeric red fluorescent protein. *Proc. Natl. Acad. Sci. USA* **99**, 7877-7882.

Cheviet, S., Coppola, T., Haynes, L. P., Burgoyne, R. D. and Regazzi, R. (2004a). The Rab-binding protein Noc2 is associated with insulin-containing secretory granules and is essential for pancreatic β-cell exocytosis. *Mol. Endocrinol.* **18**, 117-126.

Cheviet, S., Waselle, L. and Regazzi, R. (2004b). Noc-king out exocrine and endocrine secretion. *Trends Cell Biol.* **14**, 525-528.

Chung, S. H., Takai, Y. and Holz, R. W. (1995). Evidence that the Rab3a-binding protein, rabphilin3a, enhances regulated secretion: studies in adrenal chromaffin cells. *J. Biol. Chem.* **270**, 16714-16718.

Coppola, T., Frantz, C., Perret-Menoud, V., Gattesco, S., Hirling, H. and Regazzi, R. (2002). Pancreatic β-cell protein granuphilin binds Rab3 and Munc-18 and controls exocytosis. *Mol. Biol. Cell* **13**, 1906-1915.

Desnos, C., Schonn, J. S., Huet, S., Tran, V. S., El Amraoui, A., Raposo, G., Fanget, I., Chapuis, C., Ménasché, G., de Saint Basile, G. et al. (2003). Rab27A and its effector MyRIP link secretory granules to F-actin and control their motion towards release sites. *J. Cell Biol.* **163**, 559-570.

Fukuda, M. (2003a). Distinct Rab binding specificity of Rim1, Rim2, rabphilin, and Noc2: identification of a critical determinant of Rab3A/Rab27A recognition by Rim2. *J. Biol. Chem.* **278**, 15373-15380.

Fukuda, M. (2003b). Slp4-a/granuphilin-a inhibits dense-core vesicle exocytosis through interaction with the GDP-bound form of Rab27A in PC12 cells. *J. Biol. Chem.* **278**, 15390-15396.

Fukuda, M. (2004). Alternative splicing in the first α-helical region of the Rab-binding domain of Rim regulates Rab3A binding activity: is Rim a Rab3 effector protein during evolution? *Genes Cells* **9**, 831-842.

Fukuda, M. (2005). Versatile role of Rab27 in membrane trafficking: focus on the Rab27 effector families. *J. Biochem. Tokyo* **137**, 9-16.

Fukuda, M. (2006). The role of synaptotagmin and synaptotagmin-like protein (Slp) in regulated exocytosis. In *Molecular Mechanisms of Exocytosis* (ed. R. Regazzi), in press (http://eurekah.com/abstract.php?chapid=2872&bookid=218&catid=15).

Fukuda, M. and Mikoshiba, K. (1999). A novel alternatively spliced variant of synaptotagmin VI lacking a transmembrane domain: implications for distinct functions of the two isoforms. *J. Biol. Chem.* **274**, 31428-31434.

Fukuda, M. and Kuroda, T. S. (2002). Slac2-c (synaptotagmin-like protein homologue lacking C2 domains-c), a novel linker protein that interacts with Rab27, myosin Va/VIIa, and actin. *J. Biol. Chem.* **277**, 43096-43103.

Fukuda, M., Kanno, E., Saegusa, C., Ogata, Y. and Kuroda, T. S. (2002). Slp4-a/granuphilin-a regulates dense-core vesicle exocytosis in PC12 cells. *J. Biol. Chem.* **277**, 39673-39678.

Fukuda, M., Kanno, E. and Yamamoto, A. (2004). Rabphilin and Noc2 are recruited to dense-core vesicles through specific interaction with Rab27A in PC12 cells. *J. Biol. Chem.* **279**, 13065-13075.

Fukuda, M., Imai, A., Nashida, T. and Shimomura, H. (2005). Slp4-a/granuphilin-a interacts with syntaxin-2/3 in a Munc18-2-dependent manner. *J. Biol. Chem.* **280**, 39175-39184.

Haddad, E. K., Wu, X., Hammer, J. A., III and Henkart, P. A. (2001). Defective granule exocytosis in Rab27a-deficient lymphocytes from *ashen* mice. *J. Cell Biol.* **152**, 835-842.

Haynes, L. P., Evans, G. J., Morgan, A. and Burgoyne, R. D. (2001). A direct inhibitory role for the Rab3-specific effector, Noc2, in Ca^{2+}-regulated exocytosis in neuroendocrine cells. *J. Biol. Chem.* **276**, 9726-9732.

Imai, A., Yoshie, S., Nashida, T., Shimomura, H. and Fukuda, M. (2004). The small GTPase Rab27B regulates amylase release from rat parotid acinar cells. *J. Cell Sci.* **117**, 1945-1953.

Jahn, R. and Südhof, T. C. (1999). Membrane fusion and exocytosis. *Annu. Rev. Biochem.* **68**, 863-911.

Kasai, K., Ohara-Imaizumi, M., Takahashi, N., Mizutani, S., Zhao, S., Kikuta, T., Kasai, H., Nagamatsu, S., Gomi, H. and Izumi, T. (2005). Rab27a mediates the tight docking of insulin granules onto the plasma membrane during glucose stimulation. *J. Clin. Invest.* **115**, 388-396.

Kotake, K., Ozaki, N., Mizuta, M., Sekiya, S., Inagaki, N. and Seino, S. (1997). Noc2, a putative zinc finger protein involved in exocytosis in endocrine cells. *J. Biol. Chem.* **272**, 29407-29410.

Kuroda, T. S. and Fukuda, M. (2004). Rab27A-binding protein Slp2-a is required for peripheral melanosome distribution and elongated cell shape in melanocytes. *Nat. Cell Biol.* **6**, 1195-1203.

Kuroda, T. S., Fukuda, M., Ariga, H. and Mikoshiba, K. (2002a). The Slp homology domain of synaptotagmin-like proteins 1-4 and Slac2 functions as a novel Rab27A binding domain. *J. Biol. Chem.* **277**, 9212-9218.

Kuroda, T. S., Fukuda, M., Ariga, H. and Mikoshiba, K. (2002b). Synaptotagmin-like protein 5, a novel Rab27A effector with C-terminal tandem C2 domains. *Biochem. Biophys. Res. Commun.* **293**, 899-906.

Lang, T., Wacker, I., Wunderlich, I., Rohrbach, A., Giese, G., Soldati, T. and Almers, W. (2000). Role of actin cortex in the subplasmalemmal transport of secretory granules in PC-12 cells. *Biophys. J.* **78**, 2863-2877.

Masuda, E. S., Luo, Y., Young, C., Shen, M., Rossi, A. B., Huang, B. C., Yu, S., Bennett, M. K., Payan, D. G. and Scheller, R. H. (2000). Rab37 is a novel mast cell specific GTPase localized to secretory granules. *FEBS Lett.* **470**, 61-64.

Nagai, T., Ibata, K., Park, E. S., Kubota, M., Mikoshiba, K. and Miyawaki, A. (2002). A variant of yellow fluorescent protein with fast and efficient maturation for cell-biological applications. *Nat. Biotechnol.* **20**, 87-90.

Pereira-Leal, J. B., Hume, A. N. and Seabra, M. C. (2001). Prenylation of Rab GTPases: molecular mechanisms and involvement in genetic disease. *FEBS Lett.* **498**, 197-200.

Pfeffer, S. R. (2001). Rab GTPases: specifying and deciphering organelle identity and function. *Trends Cell Biol.* **11**, 487-491.

Regazzi, R., Ravazzola, M., Iezzi, M., Lang, J., Zahraoui, A., Andereggen, E., Morel, P., Takai, Y. and Wollheim, C. B. (1996). Expression, localization and functional role of small GTPases of the Rab3 family in insulin-secreting cells. *J. Cell Sci.* **109**, 2265-2273.

Rothman, J. E. (1994). Mechanisms of intracellular protein transport. *Nature* **372**, 55-63.

Segev, N. (2001). Ypt and Rab GTPases: insight into functions through novel interactions. *Curr. Opin. Cell Biol.* **13**, 500-511.

Shirataki, H., Kaibuchi, K., Sakoda, T., Kishida, S., Yamaguchi, T., Wada, K., Miyazaki, M. and Takai, Y. (1993). Rabphilin-3A, a putative target protein for smg p25A/rab3A p25 small GTP-binding protein related to synaptotagmin. *Mol. Cell. Biol.* **13**, 2061-2068.

Stinchcombe, J. C., Barral, D. C., Mules, E. H., Booth, S., Hume, A. N., Machesky, L. M., Seabra, M. C. and Griffiths, G. M. (2001). Rab27a is required for regulated secretion in cytotoxic T lymphocytes. *J. Cell Biol.* **152**, 825-834.

Sun, L., Bittner, M. A. and Holz, R. W. (2001). Rab3a binding and secretion-enhancing domains in Rim1 are separate and unique: studies in adrenal chromaffin cells. *J. Biol. Chem.* **276**, 12911-12917.

Torii, S., Takeuchi, T., Nagamatsu, S. and Izumi, T. (2004). Rab27 effector granuphilin promotes the plasma membrane targeting of insulin granules via interaction with syntaxin 1a. *J. Biol. Chem.* **279**, 22532-22538.

Tsuboi, T. and Rutter, G. A. (2003). Multiple forms of "kiss-and-run" exocytosis revealed by evanescent wave microscopy. *Curr. Biol.* **13**, 563-567.

Tsuboi, T. and Fukuda, M. (2005). The C2B domain of rabphilin directly interacts with SNAP-25 and regulates the docking step of dense-core vesicle exocytosis in PC12 cells. *J. Biol. Chem.* **280**, 39253-39259.

Tsuboi, T., Zhao, C., Terakawa, S. and Rutter, G. A. (2000). Simultaneous evanescent wave imaging of insulin vesicle membrane and cargo during a single exocytotic event. *Curr. Biol.* **10**, 1307-1310.

Tsuboi, T., da Silva-Xavier, G., Leclerc, I. and Rutter, G. A. (2003). 5′-AMP-activated protein kinase controls insulin-containing secretory vesicle dynamics. *J. Biol. Chem.* **278**, 52042-52051.

Tsuboi, T., McMahon, H. T. and Rutter, G. A. (2004). Mechanisms of dense core vesicle recapture following "kiss and run" ("cavicapture") exocytosis in insulin-secreting cells. *J. Biol. Chem.* **279**, 47115-47124.

Tsuboi, T., Ravier, M. A., Xie, H., Ewart, M. A., Gould, G. W., Baldwin, S. A. and Rutter, G. A. (2005). Mammalian exocyst complex is required for the docking step of insulin vesicle exocytosis. *J. Biol. Chem.* **280**, 25565-25570.

Waselle, L., Coppola, T., Fukuda, M., Iezzi, M., El Amraoui, A., Petit, C. and Regazzi, R. (2003). Involvement of the Rab27 binding protein Slac2c/MyRIP in insulin exocytosis. *Mol. Biol. Cell* **14**, 4103-4113.

Yi, Z., Yokota, H., Torii, S., Aoki, T., Hosaka, M., Zhao, S., Takata, K., Takeuchi, T. and Izumi, T. (2002). The Rab27a/granuphilin complex regulates the exocytosis of insulin-containing dense-core granules. *Mol. Cell. Biol.* **22**, 1858-1867.

Zerial, M. and McBride, H. (2001). Rab proteins as membrane organizers. *Nat. Rev. Mol. Cell Biol.* **2**, 107-117.

Zheng, J. Y., Koda, T., Fujiwara, T., Kishi, M., Ikehara, Y. and Kakinuma, M. (1998). A novel Rab GTPase, Rab33B, is ubiquitously expressed and localized to the medial Golgi cisternae. *J. Cell Sci.* **111**, 1061-1069.